

Dynamic Light Scattering Study on the Calf Vitreous Body

Toyoaki Matsuura,[†] Yoshiaki Hara,[†] Sinnji Maruoka,[†] Shinsuke Kawasaki,[†] Shigeo Sasaki,[‡] and Masahiko Annaka^{*,‡}

Department of Ophthalmology, Nara Medical University, 840, Shijyo-cho, Kashihara-shi, Nara 634-8522, Japan, and Department of Chemistry, Faculty of Science, Kyushu University, 6-10-1, Hakozaki, Higashi-ku, Fukuoka-shi, Fukuoka 812-8581, Japan

Received June 22, 2004; Revised Manuscript Received August 5, 2004

ABSTRACT: From the observations of the dynamics of light scattered by the calf vitreous body, intensity autocorrelation functions that revealed two diffusion coefficients, D_{fast} and D_{slow} , were obtained. We developed the theory for describing the density fluctuation of the entities in the vitreous gel system with Na-hyaluronate polymers filled in the meshes of collagen fiber network. The dynamics of collagen and Na-hyaluronate explains two relaxation modes of the fluctuation. The diffusion coefficient of collagen obtained from D_{fast} and D_{slow} is very close to that in aqueous solution, which suggests the vitreous body is in the swollen state. The diffusion coefficients were found to be dependent on the position (surface or central part) of the vitreous body from which the scattered light sampled. The inhomogeneous distribution of Na-hyaluronate and collagen and the shell structure of the vitreous body were suggested.

1. Introduction

The vitreous body is a tenuous gel that contains collagen and Na-hyaluronate.¹ The fraction of the polymer network is only about 1–2%, and the remaining is water. Therefore, a large amount of water is sustained within the dilute polymer network. The vitreous body is located between the lens and the retina that comprises 80% of the overall volume of eye. The functions of the vitreous body are supposed to keep the shape of the eyeball, to absorb the external mechanical shock, to maintain the homeostasis of the eye, and to regulate the position of the lens. The appearance of fresh vitreous body is transparent, and hence, the vitreous body is considered a uniform tissue. These functions of the vitreous body are still under controversy.

A critical juncture in the advancement of gel research was the realization that scattered light intensity fluctuations, arising from concentration or density fluctuations within gels, represented thermally excited acoustic and elastic vibrations of the gel matrix (phonons) that are rapidly dampened by frictional forces.² Subsequent light scattering experiments were able to verify that (1) the magnitude of the scattered light intensity fluctuations was dependent upon the compressibility of the gel network, (2) the ratio of the elastic modulus and frictional coefficient of the network in its fluid medium, or the effective pore size of the network, can be determined by the collective diffusion coefficients of gels obtained from the decay times of the intensity correlation functions, and (3) as the gel approaches the critical points, critical phenomena can be evidenced in the form of the divergent behavior in the observed scattered light intensities and the collective diffusion coefficients of gels.³

The vitreous body has a complex structure, in which the highly flexible Na-hyaluronate is considered to be interwoven by semirigid network of collagen threads.

Many studies performed to date have suggested that Na-hyaluronate, which has a coil shape, is uniformly distributed throughout the three-dimensional network of collagen fibers that form the triple helix in the vitreous body.⁴ However, the structural properties of the vitreous body have not been determined. And essentially no investigations on the dynamics and phase equilibrium properties of the vitreous body, however, have been performed to verify indisputably that the vitreous body is indeed a gel network.

Some diseases affect changes in the complex structure of the vitreous body. The collapse of the vitreous body may cause many diseases such as posterior vitreous detachment, vitreous bleeding, and retinal detachment.^{5,6} In the search for the underlying principle of the functions of the vitreous body, it is crucial to understand its physical properties, which leads to promote better understanding of the mechanism of diseases of the vitreous body.

In this study, the microscope laser light scattering spectroscopy is applied to investigate the structural and dynamical properties of the gel network in the calf vitreous body. It is natural to consider the collagen motion is coupled with the dynamics of Na-hyaluronate; therefore, we develop the equation for the mode coupling of flexible Na-hyaluronate and semirigid network of collagen.

The unique physical properties of a gel arise from its structure. The gel is characterized by two kinds of bulk coefficients: (1) the elastic constants of the gel network and (2) the friction coefficients between gel network and the fluid. We determine the friction coefficients between vitreous gel network and gel fluid using a specially designed apparatus.⁷ Together with experimental and theoretical results of dynamic light scattering (DLS), we discuss the elastic properties of the calf vitreous body.

2. Theory for the Density Fluctuation of Complex System of Polymers Filling in the Network Meshes

The situation that Na-hyaluronate polymers fill in the meshes of collagen fiber network to prevent them from

[†] Nara Medical University.

[‡] Kyushu University.

* To whom correspondence should be addressed: Fax +81-92-642-2594; e-mail annaka-scc@mbox.nc.kyushu-u.ac.jp.

collapsing can be modeled as a complex system of polymers interacting with the network meshes. The DLS measures the time correlation of density fluctuation of the scattering entities, which are the segments of the Na-hyaluronate polymer and the collagen mesh. The concentration fluctuation of the Na-hyaluronate polymer segment, $\delta C_{HA}(\mathbf{r}, t) (= C_{HA}(\mathbf{r}, t) - C_{HA}^0)$, where $C_{HA}(\mathbf{r}, t)$ and C_{HA}^0 respectively are the local and the averaged concentrations of the segment, can be described by the following diffusion equation:⁸

$$\frac{\partial \delta C_{HA}(\mathbf{r}, t)}{\partial t} = D_{HA} \nabla^2 \delta C_{HA}(\mathbf{r}, t) + L_{HA-Col} D_H \frac{C_{HA}^0}{C_{Col}^0} \nabla^2 \delta C_{Col}(\mathbf{r}, t) \quad (1)$$

where D_{HA} and L_{HA-Col} respectively are a diffusion coefficient defined in the interparticle interaction free condition and a phenomenological coefficient, which is significant in the case that the acting force of collagen matrix on the Na-hyaluronate polymer is large. The subscripts, HA and Col, denote hyaluronic acid and collagen, respectively. Here, C_{Col}^0 and $\delta C_{Col}(\mathbf{r}, t)$ respectively are the averaged concentration and the concentration fluctuation of the collagen segment. The collagen network can be regarded as an elastic body. According to the linear theory for the elastic body, a force balance among elastic and the external forces can be described by the following Newton equation:

$$\rho \frac{\partial^2 \mathbf{u}}{\partial t^2} = \mu \nabla^2 \mathbf{u} + \left(K + \frac{1}{3} \mu \right) \nabla (\nabla \cdot \mathbf{u}) - f \frac{\partial \mathbf{u}}{\partial t} + \mathbf{F}_{Col} \quad (2)$$

where ρ , \mathbf{u} , μ , K , f , and \mathbf{F}_{Col} respectively are the density of the network, a displacement vector of the collagen segment, a shear modulus, a bulk modulus, a friction coefficient of an unit volume, and the force acted by the hyaluronate polymer. The inertia term is negligibly small in the fluctuation, that is, $\rho \partial^2 \mathbf{u} / \partial t^2 = 0$. Then eq 2 leads to

$$\frac{\partial \delta C_{Col}(\mathbf{r}, t)}{\partial t} = D_S \nabla^2 \delta C_{Col}(\mathbf{r}, t) + L_{Col-HA} D_{Col} \frac{C_{Col}^0}{C_{HA}^0} \nabla^2 \delta C_{HA}(\mathbf{r}, t) \quad (3)$$

where

$$D_S = (K + 4\mu/3)/f \quad (3.1)$$

$$D_{Col} = (T/f) C_{Col}^0 \quad (3.2)$$

and L_{Col-HA} is a phenomenological coefficient related to the acting force of Na-hyaluronate polymer on collagen matrix. Here T is the Boltzmann temperature. Here we use units where Boltzmann's constant k_B is unity to use energy units for temperature. In deriving eq 3, the following relations are used:

$$C_{Col}^0 \nabla \cdot \mathbf{u}(\mathbf{r}) + \delta C_{Col}(\mathbf{r}, t) = 0 \quad (3.3)$$

$$\mathbf{F}_{Col} = -L_{Col-HA} T C_{Col}(\mathbf{r}, t) \nabla \ln C_{HA}(\mathbf{r}, t) \quad (3.4)$$

and

$$f = C_{Col}^0 \zeta_{Col} \quad (3.5)$$

where ζ_{Col} is a friction coefficient of the collagen segment. Equations 1 and 3 can be rewritten in the form of Fourier transform of the concentrations as

$$\frac{\partial C_{HA}(q, t)}{\partial t} = -q^2 \left\{ D_{HA} C_{HA}(q, t) + L_{HA-Col} D_{HA} \frac{C_{HA}^0}{C_{Col}^0} C_{Col}(q, t) \right\} \quad (4)$$

$$\frac{\partial C_{Col}(q, t)}{\partial t} = -q^2 \left\{ D_S C_{Col}(q, t) + L_{Col-HA} D_{Col} \frac{C_{Col}^0}{C_{HA}^0} C_{HA}(q, t) \right\} \quad (5)$$

where

$$\delta C_{HA}(\mathbf{r}, t) = \left(\frac{1}{2\pi} \right)^3 \int \int \int d\mathbf{r}^3 C_{HA}(\mathbf{q}, t) \exp(i\mathbf{q} \cdot \mathbf{r})$$

and

$$\delta C_{Col}(\mathbf{r}, t) = \left(\frac{1}{2\pi} \right)^3 \int \int \int d\mathbf{r}^3 C_{Col}(\mathbf{q}, t) \exp(i\mathbf{q} \cdot \mathbf{r})$$

Equations 4 and 5 can be converted into matrix form as

$$\frac{\partial}{\partial t} \mathbf{C}(\mathbf{q}) = -q^2 \tilde{A} \mathbf{C}(\mathbf{q}) \quad (6)$$

where

$$\mathbf{C}(\mathbf{q}) = \begin{pmatrix} C_{HA}(\mathbf{q}, t) \\ C_{Col}(\mathbf{q}, t) \end{pmatrix} \quad \text{and} \quad \tilde{A} = \begin{pmatrix} D_{HA} & L_{HA-Col} D_{HA} \frac{C_{HA}^0}{C_{Col}^0} \\ L_{Col-HA} D_{Col} \frac{C_{Col}^0}{C_{HA}^0} & D_S \end{pmatrix}$$

The solution of eq 6 is given as

$$\begin{pmatrix} C_{HA}(\mathbf{q}, t) \\ C_{Col}(\mathbf{q}, t) \end{pmatrix} = B(\mathbf{q}) \begin{pmatrix} D_1(\mathbf{q}) \exp(-q^2 \lambda_1 t) \\ D_2(\mathbf{q}) \exp(-q^2 \lambda_2 t) \end{pmatrix}$$

where

$$\tilde{B}^{-1}(\mathbf{q}) \tilde{A}(\mathbf{q}) \tilde{B}(\mathbf{q}) = \begin{pmatrix} \lambda_1 & 0 \\ 0 & \lambda_2 \end{pmatrix}$$

with

$$2\lambda_{1 \text{ or } 2} = D_{HA} + D_S \pm [(D_{HA} - D_S)^2 + 4D_{HA} L_{Col-HA} A D_{Col} L_{HA-Col}]^{1/2} \quad (\lambda_1 \geq \lambda_2) \quad (7)$$

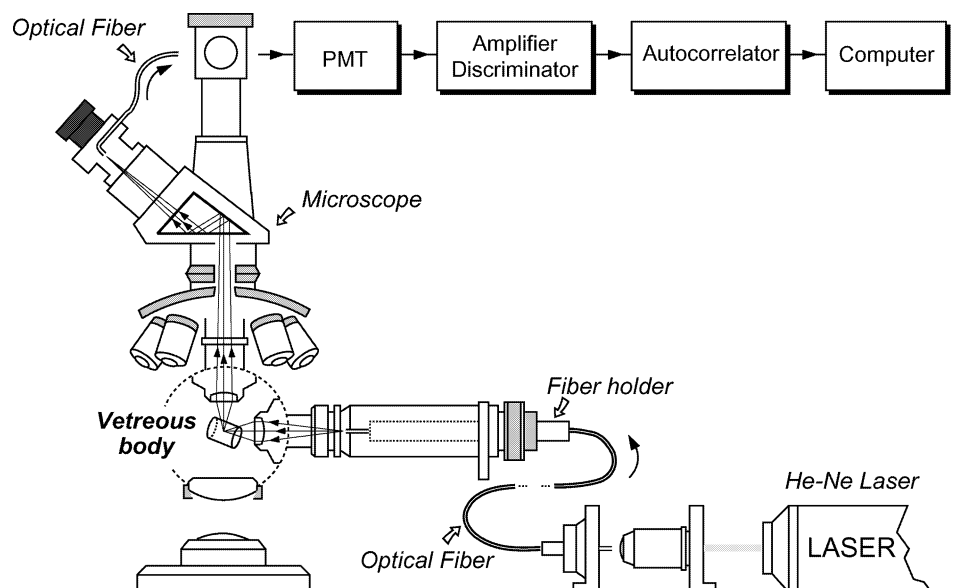


Figure 1. Schematic illustration of the microscope laser light scattering spectroscopy (MLLSS).

and

$$\tilde{B} \approx \frac{1}{\sqrt{D_{\text{HA}} L_{\text{Col-HA}} D_{\text{Col}} L_{\text{HA-Col}} + \Delta D^2}} \times \begin{pmatrix} L_{\text{Col-HA}} D_{\text{Col}} \frac{C_{\text{Col}}^0}{C_{\text{HA}}^0} \Delta D \\ -\Delta D & L_{\text{HA-Col}} D_{\text{HA}} \frac{C_{\text{HA}}^0}{C_{\text{Col}}^0} \end{pmatrix}$$

$$\tilde{B}^{-1} \approx \frac{1}{\sqrt{D_{\text{HA}} L_{\text{Col-HA}} D_{\text{Col}} L_{\text{HA-Col}} + \Delta D^2}} \times \begin{pmatrix} L_{\text{HA-Col}} D_{\text{H}} \frac{C_{\text{HA}}^0}{C_{\text{Col}}^0} - \Delta D \\ \Delta D & L_{\text{Col-HA}} D_{\text{Col}} \frac{C_{\text{Col}}^0}{C_{\text{HA}}^0} \end{pmatrix}$$

$$\Delta D = \frac{|D_{\text{S}} - D_{\text{HA}}|}{2} \left\{ 1 - \sqrt{1 + 4 D_{\text{HA}} L_{\text{Col-HA}} D_{\text{Col}} L_{\text{HA-Col}} (D_{\text{HA}} - D_{\text{S}})^{-2}} \right\} \quad (8)$$

Thus, concentration fluctuation can be given by

$$C_{\text{HA}}(\mathbf{q}, t) \propto L_{\text{Col-HA}} D_{\text{Col}} \frac{C_{\text{Col}}^0}{C_{\text{HA}}^0} \exp(-q^2 \lambda_1 t) + \Delta D \exp(-q^2 \lambda_2 t) \quad (9)$$

$$C_{\text{Col}}(\mathbf{q}, t) \propto -\Delta D \exp(-q^2 \lambda_1 t) + L_{\text{HA-Col}} D_{\text{H}} \frac{C_{\text{HA}}^0}{C_{\text{Col}}^0} \exp(-q^2 \lambda_2 t) \quad (10)$$

Finally, eq 10 yields a double exponentially decaying function for the time correlation of the electric field

of scattering light as follows:

$$g^{(1)}(q, \tau) \propto A_{\text{fast}} \exp(-q^2 \lambda_1 \tau) + A_{\text{slow}} \exp(-q^2 \lambda_2 \tau) \quad (11)$$

where A_{fast} and A_{slow} are constants.

3. Experimental Section

3.1. Materials. The vitreous body of the calf eye was chosen for our study because it is easily obtained and handled. Calf vitreous body was isolated from sclera of the eyeball. The choroid membrane was also carefully removed by the standard method.⁹ The sample preparation was performed within 8 h after extraction of the eye at a local slaughterhouse.

3.2. Microscope Laser Light Scattering Spectroscopy. Since the vitreous body is difficult to hold in a sample cell, we used the technique of the microscope laser light scattering spectroscopy (MLLSS). The technique differs from the conventional dynamic laser light scattering technique in that the scattering volume in the MLLSS is some 10^5 times smaller, making it as low as $2 \mu\text{m}^3$. It, therefore, becomes possible to analyze the motion of particles inside the vitreous body. The schematic diagram of the MLLSS setup is illustrated in Figure 1.^{10,11} The beam of a He-Ne laser (632.8 nm, Spectra Physics 124A) was focused onto the equatorial plane of the vitreous body through an optical fiber connected to the fiber coupler that is equipped with a condensing lens. The beam is sharply focused onto the various positions of the vitreous body placed under an upright microscope (Nikon Optiphot). The cross section at the focal point within the vitreous body was approximately $2 \times 2 \mu\text{m}$. The focal region was imaged onto a photomultiplier tube (EMI 9863B-350) by a $50 \mu\text{m}$ diameter optical fiber embedded in one of the eyepieces of the microscope (Gamma Scientific 700-10-36A). The fluctuations of the number of photons were analyzed using the autocorrelator (Brookhaven Instrument, model BI-2030A).

The temporal fluctuations of the scattered light intensity $I(t)$ were analyzed in terms of intensity autocorrelation functions^{12,13}

$$C(\tau) = \langle I(t) \cdot I(t + \tau) \rangle_t \quad (12)$$

where $\langle \rangle$ stands for the time average over t . The rate of the fluctuations of the scattered light intensity, which represent the density fluctuations of the vitreous gel, is proportional to the rate of local swelling and shrinking of the gel via molecular Brownian motions. There are also permanent and static inhomogeneities within the vitreous that also contribute to

light scattering. The light intensity scattered by these inhomogeneities does not fluctuate with time. The scattered light intensity is, thus, the superposition of contributions from scattering elements that are static from those that dynamically fluctuate:

$$I(t) = I_S + I_D(t) \quad (13)$$

In dynamic light scattering the time correlation of the intensity of scattered light is recorded. Assuming the Gaussian nature of the scattered light photons, the correlation function of the intensity of scattered light is rewritten in terms of the autocorrelation function $g(\tau)$ of the scattered electric field $E(t)$, which is related to the scattered light intensity: $I(t) = E(t)E^*(t)$

$$g(\tau) \equiv \frac{\langle E(t) E^*(t + \tau) \rangle_t}{\langle E(t) E^*(t) \rangle_t} \quad (14)$$

Then $C(\tau)$ is written as

$$C(\tau) = (I_S + I_D)^2 + A\{I_D^2 g^2(\tau) + 2I_S I_D g(\tau)\} \quad (15)$$

where A is the efficiency parameter of the apparatus, which is uniquely determined by the optical configuration of the setup, the value I , and the average intensities scattered by the gel fluctuations and the static inhomogeneities. For the present experiments, A was determined to be 0.8.

The electric field autocorrelation function $g(\tau)$ can be easily extracted from the intensity autocorrelation function $C(\tau)$ from knowledge of the initial value $C(0)$, the baseline $C(\infty)$, and the coefficient A , using the above relations. As we shall see later and as shown in Figure 3, the autocorrelation functions can have a distinct double-exponential feature. This indicates the presence of two different modes within the gel. Therefore, the correlation functions $g(\tau)$ are analyzed using the following relationship:

$$g(\tau) = \frac{A_{\text{fast}}}{A_{\text{fast}} + A_{\text{slow}}} \exp(-D_{\text{fast}} q^2 \tau) + \frac{A_{\text{slow}}}{A_{\text{fast}} + A_{\text{slow}}} \exp(-D_{\text{slow}} q^2 \tau) \quad (16)$$

where A_{fast} and A_{slow} are the amplitudes and D_{fast} and D_{slow} the diffusion coefficients of the fast and slow components in the bimodal distribution, respectively. The wavenumber q is defined by the scattering angle θ , the wavelength λ of the laser beam in the vitreous body, and the refractive index n :

$$q = \frac{4\pi n}{\lambda} \sin\left(\frac{\theta}{2}\right) \quad (17)$$

In the present experiments, q was approximately $6.3 \times 10^5 \text{ cm}^{-1}$.

3.3. Measurement of Friction Coefficient. The principle of the measurement of the friction coefficient of a vitreous body is schematically shown in Figure 2. The apparatus was originally designed by Tokita and Tanaka, and they determined the friction coefficients of poly(acrylamide) gel and poly(*N*-isopropylacrylamide) gel accurately under various conditions.⁷ A vitreous body of thickness d is fixed to the wall by silicon glue, and water is pushed through the vitreous body with a small pressure P . The average velocity of the water flow through the openings inside the gel, v , is determined by measuring the rate at which water flows out of the vitreous body in a steady state. The friction coefficient, f , is defined as

$$f = \frac{P}{dv} \quad (18)$$

The chromatography column with 50 cm length is used as a reservoir of water to generate the hydrostatic pressure. The range of the height of the water column can be changed from

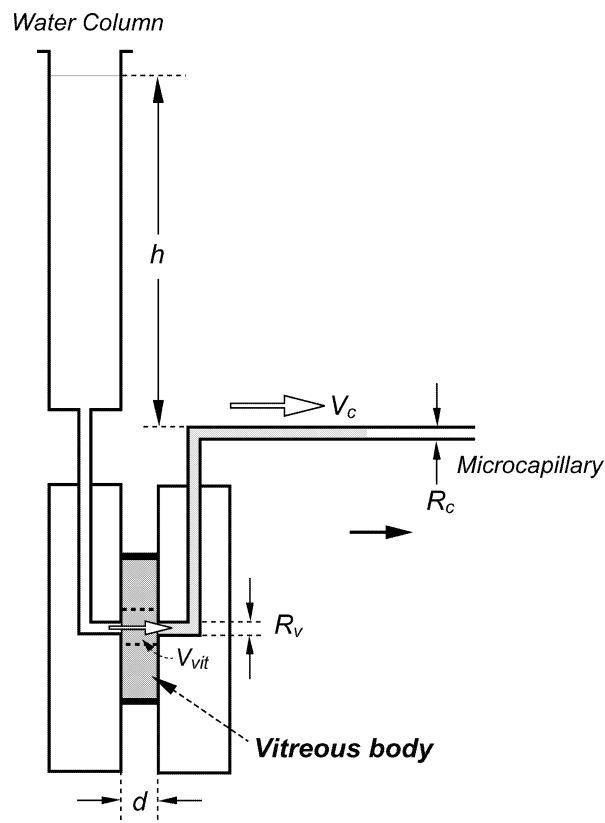


Figure 2. Schematic diagram of the apparatus for the measurement between the gel network and water. The sample mold is tightly held between two plexiglass plates. The velocity of the fluid flow in the micropipet is measured by a movable microscope with an accuracy of 0.001 mm.

20 to 60 cm, which corresponds to the pressure from 2×10^4 to $6 \times 10^4 \text{ dyn/cm}^2$. The temperature of the sample is controlled within an accuracy 0.1 °C. The apparatus is set on the vibration-free table to avoid any external mechanical disturbances. The rate of water flow through the gel was determined by measuring the movement of the water meniscus in a micropipet under a microscope.

4. Results

4.1. Dynamic Light Scattering. Figure 3 shows a correlation function obtained by MLLSS from the core region (position B in Figure 4), observed at a scattering angle 135° and at a temperature of 23 °C. From nonlinear least-squares fit to data using eqs 15–17 (the solid line in Figure 3), the essential parameters for the diffusion coefficients $D_{\text{fast}} = 5.9 \times 10^{-8} \text{ cm}^2/\text{s}$ and $D_{\text{slow}} = 3.0 \times 10^{-9} \text{ cm}^2/\text{s}$ which represent the two apparent, collective diffusion motions of the vitreous body, designated as fast and slow motions, respectively, were derived. The relative contributions of the fast and slow components to the overall dynamic scattered light intensity I_D were designated as $\%A_{\text{fast}}$ and $\%A_{\text{slow}}$, respectively, where $\%A_{\text{fast}} = 100 \times A_{\text{fast}}/(A_{\text{fast}} + A_{\text{slow}})$. The static $\%I_S$ and dynamic $\%I_D$ components of scattered light intensities, where $\%I_D = 100 \times I_D/(I_D + I_S)$, to the total scattered light intensity $I(t)$ observed at particular wave vector were also determined. For the data shown in Figure 3, $\%A_{\text{fast}} \approx 40$ and $\%I_D \approx 50$.

In the normal vitreous body, the values of the diffusion coefficients exhibited the position dependency. Table 1 summarizes the result of DLS regarding the dependence of the observed dynamics upon the position within the vitreous body, as indicated in Figure 4. Each

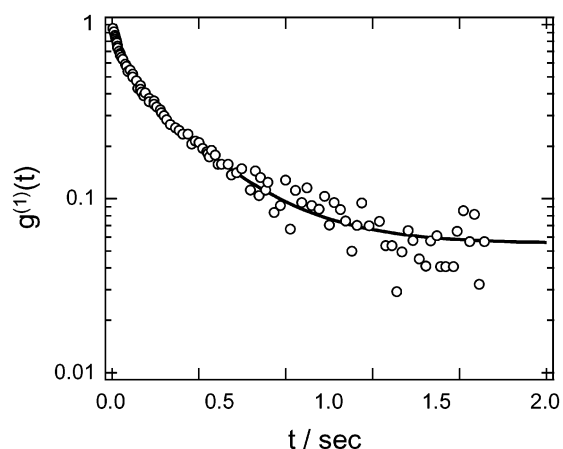


Figure 3. A correlation function as determined by the technique of MLLSS from light scattered by the calf vitreous body (position B indicated in Figure 4). The data were collected using a scattered light collection angle 135° and at a temperature 23°C . The solid line represents a computer-generated fit to the data using eqs 15–17. The results of the fit yielded for the “fast” mode $D_{\text{fast}} = 5.9 \times 10^{-8} \text{ cm}^2/\text{s}$, the “slow” mode $D_{\text{slow}} = 3.0 \times 10^{-9} \text{ cm}^2/\text{s}$, and $\%A_{\text{fast}} \approx 40$.

data is the average value of five measurements. In the surface part of the vitreous body (positions A and C), the diffusion coefficient is larger than that in the core region (B). Swann and Constable¹⁴ reported the inhomogeneous distribution of Na-hyaluronate and collagen, and the vitreous body has the shell structure: the surface part has a higher concentration compared with its central part, which serves the mechanical stabilization of the vitreous body. These facts well correspond to the experimental results obtained here.

3.2. Friction Coefficient. The velocity of the water in the micropipet at the stationary state, V_c , is obtained by measuring the shift of water meniscus for a given period of time using a movable microscope with an accuracy of 0.001 mm. The velocity thus obtained is plotted as a function of the pressure in Figure 5. At

relatively high pressures, the water flow in the vitreous body is high. Presumably, the network structure of the vitreous body is broken under high pressure; therefore, we chose five points measured at lower pressure to calculate the friction coefficients. The relationship between the applied pressure and the velocity is linear at lower pressures as predicted. The friction coefficient between vitreous body and water, $f = 6.4 \times 10^9 \text{ dyn}\cdot\text{s}/\text{cm}^4$, was obtained from the slope of the straight line in Figure 5 using the following equation:

$$f = \left(\frac{dV_c}{dp} \right)^{-1} \frac{1}{d} \left(\frac{R_v}{R_c} \right)^2 \quad (19)$$

where $dV_c/dp = 3.1 \times 10^{-8} \text{ cm}^3/(\text{dyn}\cdot\text{s})$ is determined from the slope of the straight line as given in Figure 5. The thickness of the sample, d , is 0.5 cm. The factor $(R_v/R_c)^2$ is the ratio of the area of the micropipet of radius $R_c = 3.4 \times 10^{-2} \text{ cm}$ and the area of the hole in the vitreous body with radius $R_v = 3.3 \times 10^{-1} \text{ cm}$, which is necessary to convert V_c to V_{vit} . The value of f measured here is from the total water flow along the orbital axis in the vitreous body. More precise measurements at difference positions are needed, but it is very difficult to measure water flow in a high-water-content vitreous body without destruction of its network structure. Therefore, we use this friction coefficient in the following discussions.

5. Discussion

The vitreous body can be regarded as a gel composed of the highly flexible Na-hyaluronate polymers. The fluid gel is interwoven by semirigid network of collagen threads which serve the mechanical stabilization of the body. As mentioned in the theoretical section, the DLS measures the time correlation of density fluctuation of the scattering entities, which are the segments of the Na-hyaluronate polymer and the collagen mesh. Synthetic gels such as poly(arylamide) gel have been known

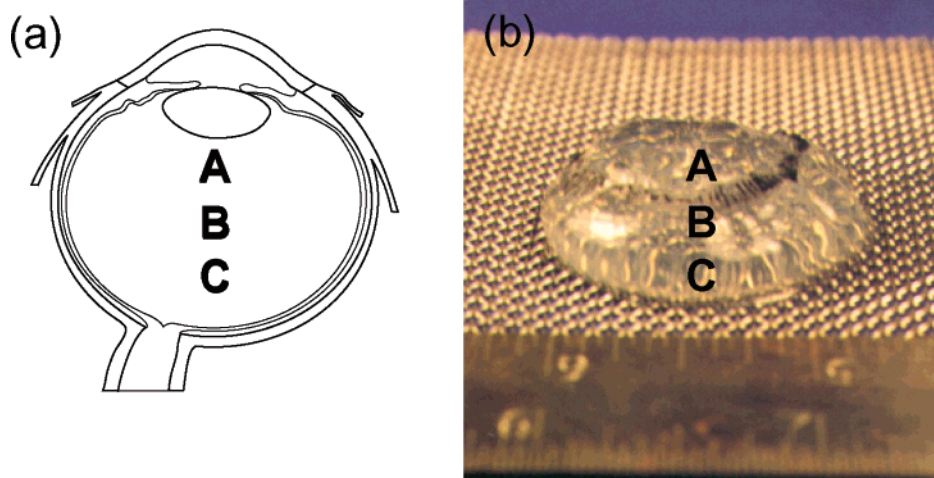


Figure 4. Cross section of the eye and the photograph of the calf vitreous body. A, B, and C indicate the sampled positions for MLLSS experiment. Positions A and C: the outer region of the vitreous body (position A corresponds to the region near the ciliary body). Position B: the central region of the vitreous body.

Table 1. Position Dependence of Dynamics of Vitreous Body

| sampled position | $\langle D_{\text{fast}} \rangle$ (cm^2/s) | $\langle D_{\text{slow}} \rangle$ (cm^2/s) | $\langle \%A_{\text{fast}} \rangle$ | $\langle \%I_D \rangle$ | $\langle \%I_S \rangle$ |
|------------------|--|--|-------------------------------------|-------------------------|-------------------------|
| A | $(10 \pm 0.98) \times 10^{-8}$ | $(4.0 \pm 0.66) \times 10^{-9}$ | 40 | 45 | 55 |
| B | $(5.9 \pm 0.83) \times 10^{-8}$ | $(3.0 \pm 0.78) \times 10^{-9}$ | 40 | 50 | 50 |
| C | $(7.8 \pm 1.52) \times 10^{-8}$ | $(3.8 \pm 0.60) \times 10^{-9}$ | 40 | 46 | 54 |

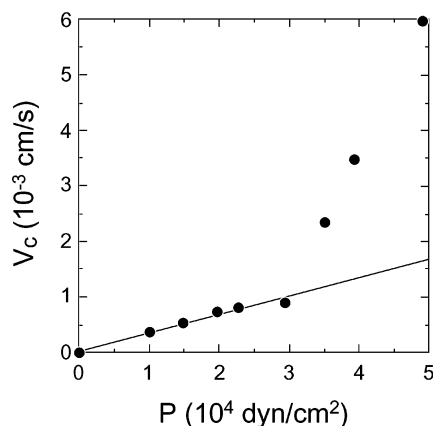


Figure 5. Velocity of water in the micropipet is plotted as a function of the water pressure. The solid line in this figure is obtained by a least-squares fit.

to show a single diffusion coefficient.³ The vitreous body, however, is found to show two different diffusion coefficient modes: one relatively fast and the other relatively slow mode. This may due to the complex structure of the vitreous body, in which the highly flexible Na-hyaluronate is interwoven by semirigid collagen threads.⁹ In this case, it is natural to consider the coupling of the collagen motion with the dynamics of Na-hyaluronate can explain the fast mode. According to eqs 11 and 7, $D_{\text{fast}} (= \lambda_1)$ and $D_{\text{slow}} (= \lambda_2)$ are given by

$$D_{\text{fast}} = D_{\text{HA}} - \Delta D \quad \text{and} \\ D_{\text{slow}} = D_{\text{S}} + \Delta D \quad (D_{\text{HA}} > D_{\text{S}}) \quad (20)$$

and

$$D_{\text{fast}} = D_{\text{S}} - \Delta D \quad \text{and} \\ D_{\text{slow}} = D_{\text{HA}} + \Delta D \quad (D_{\text{HA}} < D_{\text{S}}) \quad (21)$$

$D_{\text{HA}} \cong 2.4 \times 10^{-8} \text{ cm}^2/\text{s}$ has been reported for the Na-hyaluronate diluted in the 0.2 M NaCl aqueous solution, the molecular weight of which is similar to that ($M_w \sim 1.4 \times 10^6$) in the calf vitreous body.¹⁵ Using this result, the values of D_{S} , ΔD , and $D_{\text{Col}}L_{\text{Col-HA}}L_{\text{HA-Col}}$ are evaluated from the obtained D_{fast} and D_{slow} values and are tabulated in Table 2. It should be mentioned that the value of $D_{\text{Col}}L_{\text{Col-HA}}L_{\text{HA-Col}}$ is very close to the reported diffusion constant of collagen with a contour length 280 nm in 0.1 N HCl aqueous solution ($D_{\text{Col}} \sim (8-9) \times 10^{-8} \text{ cm}^2/\text{s}$).¹⁶ It is plausible that the $L_{\text{Col-HA}}L_{\text{HA-Col}}$ value for the collagen strongly coupled to Na-hyaluronate in the vitreous body is an order of magnitude 1. It can be inferred, therefore, that the collective diffusion coefficient of collagen in the vitreous body is very close to that in the aqueous solution. This can be realized in the highly swollen vitreous body which has enough space for the polymer segments to move freely.

It should be mentioned that the q -dependency experiment must be needed to confirm the observed two modes are diffusive. However, unfortunately, we could not conduct the further experiments using the calf vitreous

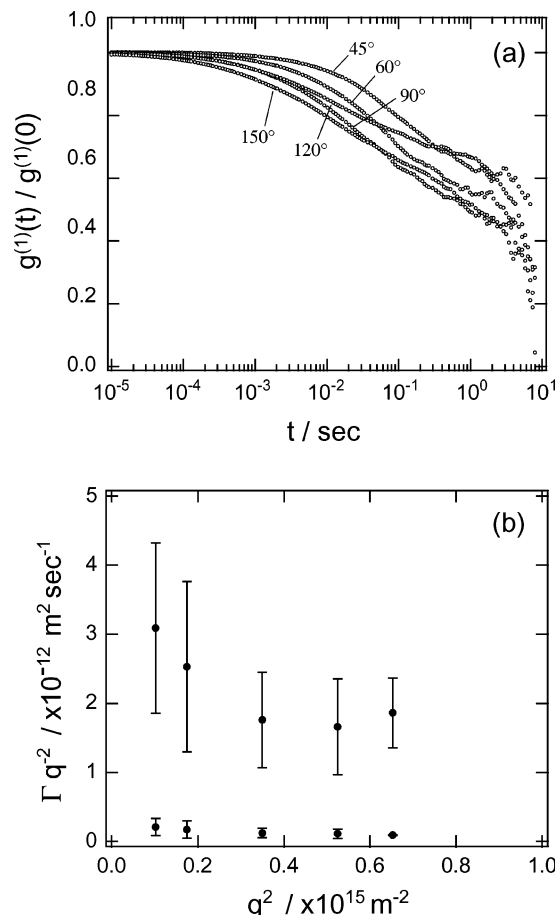


Figure 6. Scattering angle dependence of normalized electric field autocorrelation function $g^{(1)}(t)/g^{(1)}(0)$ vs t (a) and the q^2 dependence of the Γq^{-2} (b) for the pig vitreous body.

body in order to avoid the danger of infection of BSE (Bovine Spongiform Encephalopathy). We, therefore, conducted q -dependency experiments by using the pig vitreous body.¹⁷ Since a pig and a cow are the mammals, the chemical composition and the structure of both vitreous bodies are basically the same. For a polydisperse system, the decay time of the correlation function can be described by a weighted sum of exponentials:¹⁸

$$g^{(1)}(t) = \int_0^{+\infty} G(\Gamma) \exp(-\Gamma t) d\Gamma \quad (22)$$

To clarify the nature of the decay rate Γ^{-1} , the q dependence of $G(\Gamma)$ was examined. Figure 6 shows (a) the scattering angle dependence of normalized electric field autocorrelation function, $g^{(1)}(t)/g^{(1)}(0)$ vs t , and (b) the q^2 dependence of the Γq^{-2} . The distribution of relaxation rates was obtained by an inverse Laplace transformation of eq 22 with the CONTIN program.¹⁹ For a diffusional mode, one expects that Γ is proportional to q^2 . For all scattering angles, the Γq^{-2} for both fast and slow modes are almost q -independent, as shown in Figure 6b. This indicates that the observed two modes are diffusive. It should be mentioned that the apparent q^2 dependence of the Γq^{-2} is within experimental error.

Table 2. Position Dependence of Calculated Values of ΔD , the Collective Diffusion Coefficient D_{S} , the Longitudinal Modulus M , and $D_{\text{Col}}L_{\text{Col-HA}}L_{\text{HA-Col}}$

| sampld position | ΔD , $10^{-8} \text{ cm}^2/\text{s}$ | D_{S} , $10^{-8} \text{ cm}^2/\text{s}$ | $M (= K + 4\mu/3)\text{Pa}$ | $D_{\text{Col}}L_{\text{Col-HA}}L_{\text{HA-Col}}$, $10^{-8} \text{ cm}^2/\text{s}$ |
|-----------------|--|--|-----------------------------|--|
| A | -2 | 8 | 510 | 6.3 |
| B | -2.1 | 3.9 | 250 | 3.2 |
| C | -2 | 6 | 380 | 4.7 |

Very slow relaxation with decay time ranging from 1 to 10 s is observed as shown in Figure 6a. The vitreous gel has a very dilute network-like structure of collagen whose interstices are filled with Na-hyaluronate. There seems to exist a very slow accordion-like movement of semirigid network of collagen threads in the vitreous gel. This could originate in the observed very slow relaxation. It is important to note that this slow relaxation, not yet well understood, is possibly generated by a different physical mechanism and is independent of the other faster modes. Therefore, for the CONTIN analysis we introduced a cutoff at 0.1 s and subtracted the nonzero baseline.²⁰ It was verified for the correlation curves that the cutoff did not influence the decay rates and amplitudes of the faster modes. But no satisfactory explanation for this slow relaxation is given here. A detailed study on the pig vitreous body is in progress now.

The elastic moduli, $M (= K + 4\mu/3)$, estimated from the D_S and f values ($f \approx 6.4 \times 10^9 \text{ dyn}\cdot\text{s}/\text{cm}^4$) using eq 3.1 are also listed in Table 2. The intraocular pressure is created by the continual renewal of fluids within the interior of the eye and is known to be within the range 1300–2600 Ps (≈ 10 –20 mmHg) under normal physiological conditions. It is clinically known that the intraocular pressure is reduced to less than 670 Ps (≈ 5 mmHg) by artificially blocking the production of aqueous humor. In this case, only the elastic modulus of the gel network is considered to contribute the intraocular pressure; therefore, our experimental results are consistent with the clinical observation.

This study represents new structural and dynamic properties of the vitreous body. The simple consideration presented here may be helpful toward understanding of physicochemical aspects of diseases. To develop a more thorough understanding of the vitreous gel, however, much more conclusive investigations are warranted under various conditions, which is the subject of future studies.

6. Conclusion

Dynamic light scattering spectroscopy was applied to investigate the structural and dynamical properties of calf vitreous body. From the observations of the dynamics of scattered light scattered by the calf vitreous body, two different diffusion coefficient modes, one relatively fast and the other relatively slow mode, were observed. The diffusion coefficients were found to show position dependency (surface or central part), which suggested the inhomogeneous distribution of Na-hyaluronate and collagen and the vitreous body has the shell structure. We developed the coupling theory in the vitreous gel system describing the coupling of the collagen motion with the dynamics of Na-hyaluronate under the assumption that Na-hyaluronate polymer was filled in the

meshes of the collagen fiber network. The calculated value of diffusion coefficient of collagen is very close to that in aqueous solution, which suggests the vitreous body is in the swollen state, and the validity of our model. In the quest of the principle behind diseases of vitreous body, more precise study, however, is needed to reveal the structural and dynamical properties of the vitreous body at the molecular level. This will open the door for the quantitative understanding of the structure and physical properties of the vitreous body.

Acknowledgment. The work was partly supported by NIH, EY05272-05 (T.M.), and a Grant-in-Aid for Scientific Research from the Ministry of Education, Science, Sports and Culture (M.A.). M.A. and T.M. acknowledge the Sumitomo Foundation for financial support. The authors thank Prof. Toyochi Tanaka for valuable discussions and suggestions.

References and Notes

- (1) Berman, E. R.; Voaden, M. In *Biochemistry of the Eye*; Smelser, G. K., Ed.; Academic Press: London, 1970; p 373.
- (2) Tanaka, T.; Hocker, L. O.; Benedek, G. B. *J. Chem. Phys.* **1973**, *59*, 5151.
- (3) Tanaka, T.; Fillmore, D. J.; Sun, S.-T.; Nishio, I.; Swislow, G. *Phys. Rev. Lett.* **1980**, *45*, 1636.
- (4) Balazs, E. A. In *New and Controversial Aspects of Retinal Detachment*; McPherson, A., Ed.; Academic Press: Philadelphia, PA, 1968; Vol. 1, p 3.
- (5) Norman, S. *J. Arch. Ophthalmol.* **1968**, *79*, 568.
- (6) William, S. T. *Tras. Am. Acad. Ophthalmol., Otolaryngol.* **1968**, *72*, 217.
- (7) Tokita, M.; Tanaka, T. *J. Chem. Phys.* **1991**, *95*, 4613.
- (8) Sasaki, S.; Schipper, F. M. J. *J. Chem. Phys.* **2001**, *115*, 4349.
- (9) Worst, J. G. F.; Los, L. I. *Cisternal Anatomy of the Vitreous*; Kugler Publications: Amsterdam, 1995; p 1.
- (10) Nishio, I.; Tanaka, T.; Sun, S.-T.; Imanishi, Y.; Ohnishi, S. T. *Science* **1983**, *220*, 1173.
- (11) Peetermans, J.; Nisio, I.; Ohnishi, S. T.; Tanaka, T. *Biophysics* **1986**, *83*, 352.
- (12) Munch, J. P.; Candau, S.; Herz, J.; Hild, G. *J. Phys. (Paris)* **1977**, *38*, 971.
- (13) Munch, J. P.; Lemarechal, P.; Candau, S. *J. Phys. (Paris)* **1977**, *38*, 1499.
- (14) Swann, D. A.; Constable, I. *Invest. Ophthalmol.* **1972**, *11*, 164.
- (15) Takahashi, R.; Kubota, K.; Kawada, M.; Okamoto, A. *Biopolymers* **1999**, *50*, 87.
- (16) Claire, K.; Pecora, R. *J. Phys. Chem. B* **1997**, *101*, 746.
- (17) The DLS experiments on pig vitreous body was conducted using a 22 mW Uniphase He–Ne laser ($\lambda = 632.8 \text{ nm}$) (San Jose, CA) as a light source and an ALV-5000/EPP correlator (Langen, Germany) at 25 °C. Pig vitreous body was treated by the same method as the vitreous body of calf as described in the Experimental Section. The sample preparation was performed within 8 h after extraction of the eye at a local slaughterhouse.
- (18) Berne, B. J.; Pecora, R. *Dynamic Light Scattering with Applications to Chemistry, Biology, and Physics*; Wiley: New York, 1976.
- (19) Provencher, S. W. *Biophys. J.* **1976**, *16*, 27.
- (20) Papadakis, C. M.; Almdal, K.; Mortensen, K.; Rittig, F.; Stepanek, P. *Macromol. Symp.* **2000**, *162*, 275.

MA048767P